Journal of Power Sources 185 (2008) 1544–1549

Contents lists available at ScienceDirect

Journal of Power Sources

journal homepage: www.elsevier.com/locate/jpowsour

Exfoliated graphite–ruthenium oxide composite electrodes for electrochemical supercapacitors

Sagar Mitra, K.S. Lokesh, S. Sampath*

Department of Inorganic and Physical Chemistry, Indian Institute of Science, Bangalore 560012, India

ARTICLE INFO

Article history:
Received 28 May 2008
Received in revised form 1 August 2008
Accepted 4 September 2008
Available online 18 September 2008

Keywords:
Supercapacitor
Composite
Exfoliated graphite
Ruthenium oxide
Binderless electrode

ABSTRACT

The performance of exfoliated graphite (EG)–ruthenium oxide (RuO_x) composites as binderless electrodes is evaluated for electrochemical capacitors (ECs). A composite of EG–RuO_x is prepared by a modified sol–gel process. The material is characterized using X-ray diffraction and microscopy. Electrochemical capacitors with the composite electrodes in the presence of aqueous sulfuric acid (H_2SO_4) electrolyte are evaluated using voltammetry, impedance and charge–discharge studies. Cyclic voltammetry reveals very stable current–voltage behaviour up to several thousands of cycles, as well as high specific capacitances, e.g., a few hundreds of farads per gram for the composite that contains 16.5 wt.% RuO_x.

1. Introduction

Electrochemical capacitors (ECs) have attracted enormous attention in recent years in view of their high and specific power. These devices are unique in terms of power storage and release in that they exhibit good performance at high pulse rates with excellent cycle-life (>10^6 cycles) [1]. Electrochemical which are also called 'supercapacitors' are known to store energy by two different mechanisms. The first mechanism is associated with the separation of electronic and ionic charge at the electrode|electrolyte interface otherwise known as the double-layer. This type of energy storage device is typically known as an 'electrochemical double-layer capacitor (EDLC)'. Activated carbon (with a surface area of 2000 $m^2\,g^{-1}$) has been reported to yield specific single electrode capacitances of the order of 40–160 $F\,g^{-1}$ [2–5]. The second charge-storage mechanism involves very fast pseudo-Faradaic reactions at the interface and capacitors based on this mechanism are named 'pseudocapacitors'. Many transition metal oxides such as NiO_2, Co_3O_4 and MnO_2 [6–11] and conducting polymers such as polypyrrole, polyaniline, polythiophene have been used to develop pseudocapacitors [12]. Amorphous and hydrated ruthenium oxide (RuO_x) is one of the well-studied materials and show a very high specific capacitance of 760 $F\,g^{-1}$ with a specific energy of 27 $Wh\,kg^{-1}$ [13–15]. Coupling double-layer capacitance with pseudocapacitance may yield different performance characteristics to those of the individual systems. Towards this direction, carbonaceous materials modified with pseudo redox active functional groups have been tried as possible candidates for electrodes in supercapacitors [16]. Various methods that have been reported in this direction include: (i) introducing surface functionalities on the carbon surface by chemical [17] or electrochemical treatment [18]; (ii) insertion of electroactive particles of transition metal oxides [14,19–21] into carbon-based materials; (iii) making composites of conducting polymer and carbon [22–26].

Exfoliated or expanded graphite (EG) is a low-density graphite with a good surface area, electrical conductivity and high temperature resistance [27]. When graphite intercalation compounds (GIC) are given a thermal shock, the intercalates vaporize and tear the layers apart that leads to an expansion in the c direction and in a puffed-up material. The EG particles can be recompressed or re-stacked in the form of any desired shape such as sheets and rods without any inert binder. The recompressed EG is a very good adsorption substrate owing to the near perfect crystallographic face. Expanded graphic is used as a sealing material, high temperature gaskets, catalyst supports and an electromagnetic shielding material [28]. There are only a few published studies on the use of EG in electrochemistry [29,30]. In this communication, we report on the preparation and characterization of a composite of exfoliated graphite (EG) and sol–gel derived ruthenium oxide ($RuO_x{\cdot}xH_2O$). This composite material is expected to have the attributes of EG as well as ruthenium dioxide. The absence of an insulating binder may lead to a material with low resistance and high stability.

* Corresponding author. Fax: +91 80 23601552.
E-mail address: sampath@ipc.iisc.ernet.in (S. Sampath).

0378-7753/$ – see front matter © 2008 Elsevier B.V. All rights reserved.
doi:10.1016/j.jpowsour.2008.09.014

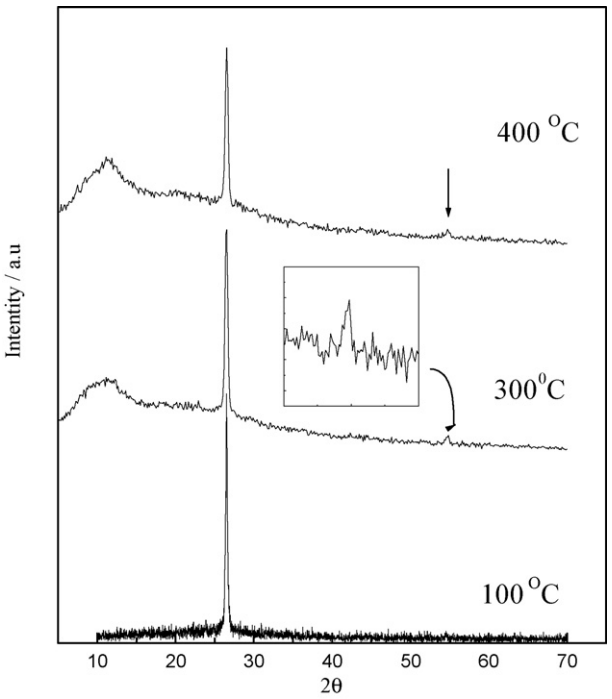

Fig. 1. X-ray diffraction patterns of 16.5 wt.% RuO_x–EG composite annealed at different temperatures.

2. Experimental

Natural graphite particles (Stratmin, NJ, USA, particle size 300–400 μm) were intercalated using a mixture of concentrated H_2SO_4:HNO_3 (3:1 by volume) for 24 h. Exfoliation was then carried out by introducing the dried material in a pre-heated furnace at 800 °C for 2 min in air. The preparation of the composite of EG and ruthenium oxide was based on a method proposed for the preparation of sol–gel derived $RuO_x{\cdot}xH_2O$ [13]. One gram of exfoliated graphite was suspended in a mixture of 1:1 (by volume) methanol:water (100 mL) containing different $RuCl_3$ (Aldrich, USA) concentrations. The mixture was then stirred for 2 h and then 1 M NaOH was added drop-wise to neutralize the solution (pH 7). During the process, ruthenium hydroxide particles precipitated out from the solution and are dispersed on the exfoliated graphite. The use of a methanol–water mixture ensured that the EG is completely wetted. The solid is then filtered off and washed well with distilled water to remove the NaCl completely. The material was dried in vacuum at room temperature for 2 h and subsequently at 150 °C for 18 h in air. The loading of ruthenium oxide was based on the mass of $RuCl_3$ used with respect to the mass of EG. The maximum loading of ruthenium oxide that could be achieved was 20%. Loadings above 20% resulted in phase separation, which may have been due to the small surface area of the EG. The electrodes were fabricated by pressing a mixture of the EG–RuO_x composite with N-methyl pyrrolidinone (NMP) as a volatile solvent on to a platinum net at a pressure of 500 kg cm^{-2}. The typical mass of the composite material used in an electrode varied between 6 and 8 mg. The thickness of the electrode was is 0.05 mm with a geometric area of 1 cm^2. All experiments were performed in an aqueous electrolyte of 0.5 M H_2SO_4 with platinum foil as the counter electrode. Cyclic voltammetry was performed in the potential range from 0 to +0.8 V, at various scan rates. Impedance measurements were carried out using a potentiostat (Model 263A, EG&G, PARC, USA) coupled to a lock-in-amplifier (Model 5210, EG&G, PARC, USA) in the frequency range 100 kHz–5 mHz. Charge–discharge measurements were carried out with a CHI 660A (TX, USA) electrochemical system. Galvanostatic charge–discharge measurements were also taken out in the potential range from 0 to 0.8 V.

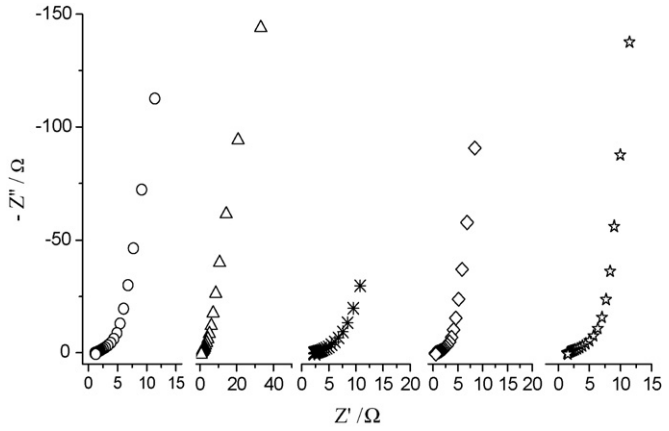

Fig. 2. Nyquist plots for various composition of RuO_x–EG composite electrodes in 0.5 M H_2SO_4, in frequency range 10^5–0.005 Hz. Impedance values given in ohms [(○) 5 wt.%; (△) 10 wt.%; (*) 14 wt.%; (□) 16.5 wt.%; (☆) 18 wt.%].

3. Results and discussion

The EG particles possess a surface area of 40 m^2 g^{-1}, whereas the compressed pellets have a surface area of (33 ± 1) m^2 g^{-1}. Scanning electron micrographs of the EG–RuO_x composite and EDAX map-

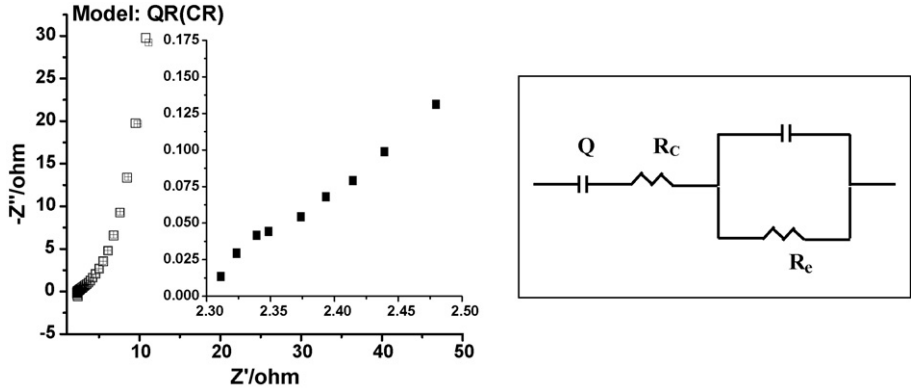

Fig. 3. (a) Equivalent circuit analysis and QR(CR) fit for Nyquist plot of 16.5 wt.% RuO_2–EG composite in three-electrode cell (□) and Z-Simpwin theoretical fit (crossed rectangles). Inset shows expanded region of Nyquist plot in high–frequency region; (b) scheme of equivalent circuit for model QR(CR).

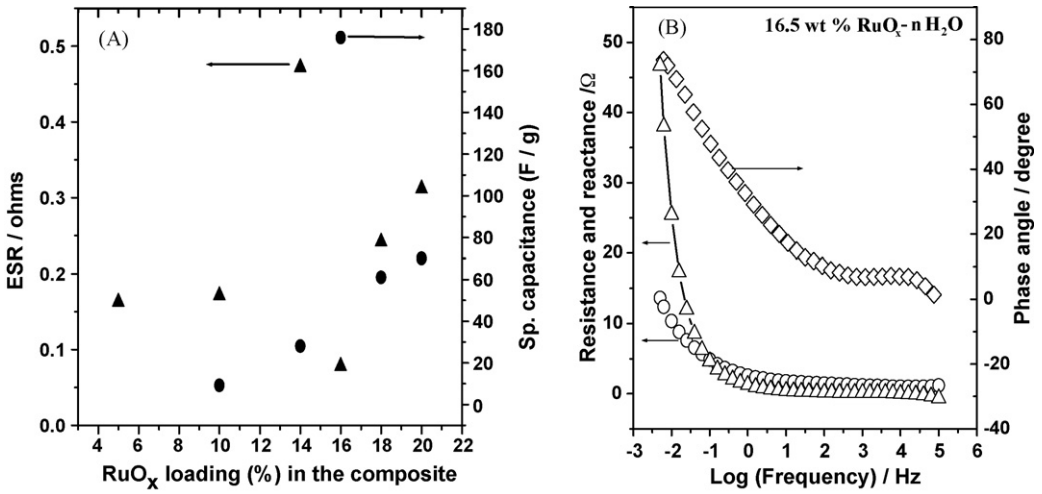

Fig. 4. (A) Equivalent series resistance (ESR) and specific capacitance versus ruthenium loading of composite electrodes in 0.5 M H_2SO_4. (B) Bode plots [(△) resistance, (○) reactance and (M) phase angle versus frequency] for 16.5 wt.% RuO_x–EG electrode in 0.5 M aqueous H_2SO_4 electrolyte.

ping show uniformly distributed ruthenium oxide particles (not shown) with a in the range of 2–10 μm depending on the loading of ruthenium in the composite. It is well documented that the crystallinity of ruthenium oxide affects capacitor performance. X-ray diffraction studies were preformed to follow the crystallinity of the ruthenium oxide particles. The experiments were conduced on EG particles loaded with 16.5 wt.% ruthenium oxide at various temperatures from 100 to 400 °C. The as-prepared composite shows

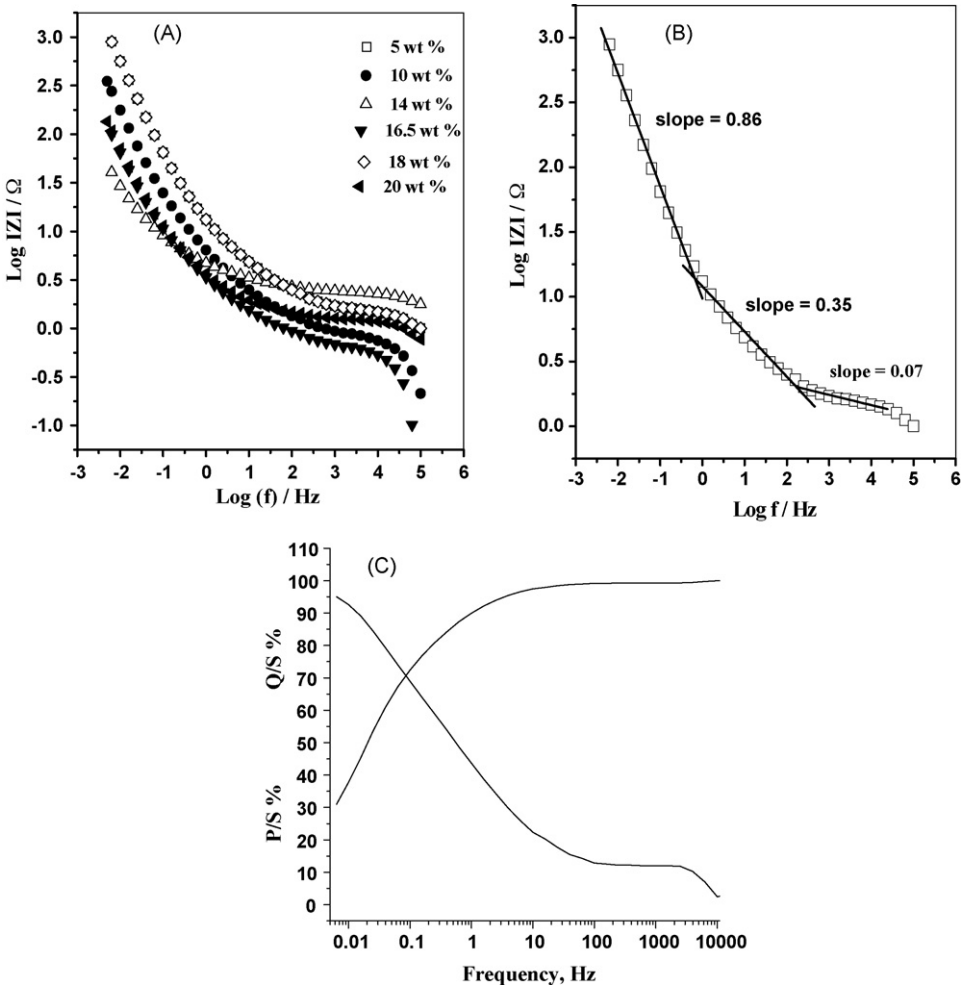

Fig. 5. (A) Bode plots of total impedance versus frequency for various compositions of RuO_x–EG electrodes in 0.5 M aqueous H_2SO_4 electrolyte. (B) Bode plot of total impedance versus frequency for 5 wt.% RuO_x–EG electrode. Different regions are shown with their slopes. (C) Normalized reactive power $|Q|/|S|$ and active power $|P|/|S|$ versus frequency plot.

an amorphous phase of $RuO_x{\cdot}xH_2O$. X-ray diffractograms (Fig. 1) of the composite treated at temperatures below 300 °C have only one intense peak that corresponds to the (0 0 2) reflection of graphite. A small peak appears at a 2θ value of 55° that corresponds to the (2 1 1) plane of crystalline RuO_2 when the composite is treated at 300 °C and above. It has been reported that $RuO_x{\cdot}xH_2O$ particles prepared by a sol–gel process are amorphous and crystalline RuO_2 appears when the samples are heated at 200 °C [13]. In the present study, the composites are heat-treated at 150 °C for 18 h to retain the amorphous nature of the samples. The specific capacitance falls to a lower value if the samples are treated at temperatures above 175 °C.

3.1. Capacitor performance

The composite electrodes were characterized by impedance spectroscopy in the frequency range 10^5 Hz–5 mHz. Nyquist plots for electrodes with different loadings of ruthenium oxide are shown in Fig. 2. The Nyquist plot shows a very small and incomplete semicircle in the high frequency region followed by a straight line. The small incomplete asymmetric semicircle observed in the high frequency region is due to the charge–transfer resistance across the electrolyte|electrode interface that is found to be very small. de Levie [31] ascribed this type of semicircle to the fractal nature of the surface and it is therefore likely that the present composite electrode has fractal dimensions as well. It has been reported that EG electrodes possess fractal geometry based on chronoamperometric measurements [30]. The impedance data is fitted to an equivalent circuit using Z-Simpwin software, as shown in Fig. 3. The high frequency semicircle is due to a charge–transfer resistance R_c associated with a capacitance of Q in parallel while the resistance R_e which, in turn, is associated with a capacitance C_e of the electrode and gives rise to a straight line at low frequencies. The constant phase element, Q, behaviour for polymer modified electrodes with a fractal nature has been reported earlier [32]. The equivalent series resistance values (ESR) are between 472 mΩ and 2.2 Ω for different loadings of RuO_2, as shown in Fig. 4A. The capacitance values normalized to the mass of the composite are also given in the same Figure. The ESR value increases with increase in the ruthenium loading and this may be due to an increase in the resistance of the matrix. The Bode phase angle plot is shown in Fig. 4B and the phase angle is observed to be close to −80° in the low-frequency range. It is well known that for a pure capacitor, the amplitude plot will give rise to a straight line with a slope of −1. In the present study, the amplitude of the total impedance versus frequency plot (Fig. 5A and B) shows three slopes at different frequency regions. The high frequency region (10^4–100 Hz) has a slope of ∼zero, whereas a slope of 0.35 is observed in the mid-frequency region (100–1 Hz). The low-frequency region (1–0.01 Hz) shows a slope of 0.86. This behaviour is explained in terms of the charge-transfer resistance or equivalent series resistance in the high frequency region, whereas the mid-frequency region comprises both the resistance and capacitor components and the low-frequency region is mainly due to the capacitive component of the interface. Plots of phase angle versus frequency also display similar behaviour (Fig. 4B).

The frequency corresponding to the region where a curves deviates from semicircular behaviour is known as the "capacitor response frequency (f_0)" and will give the response time of the

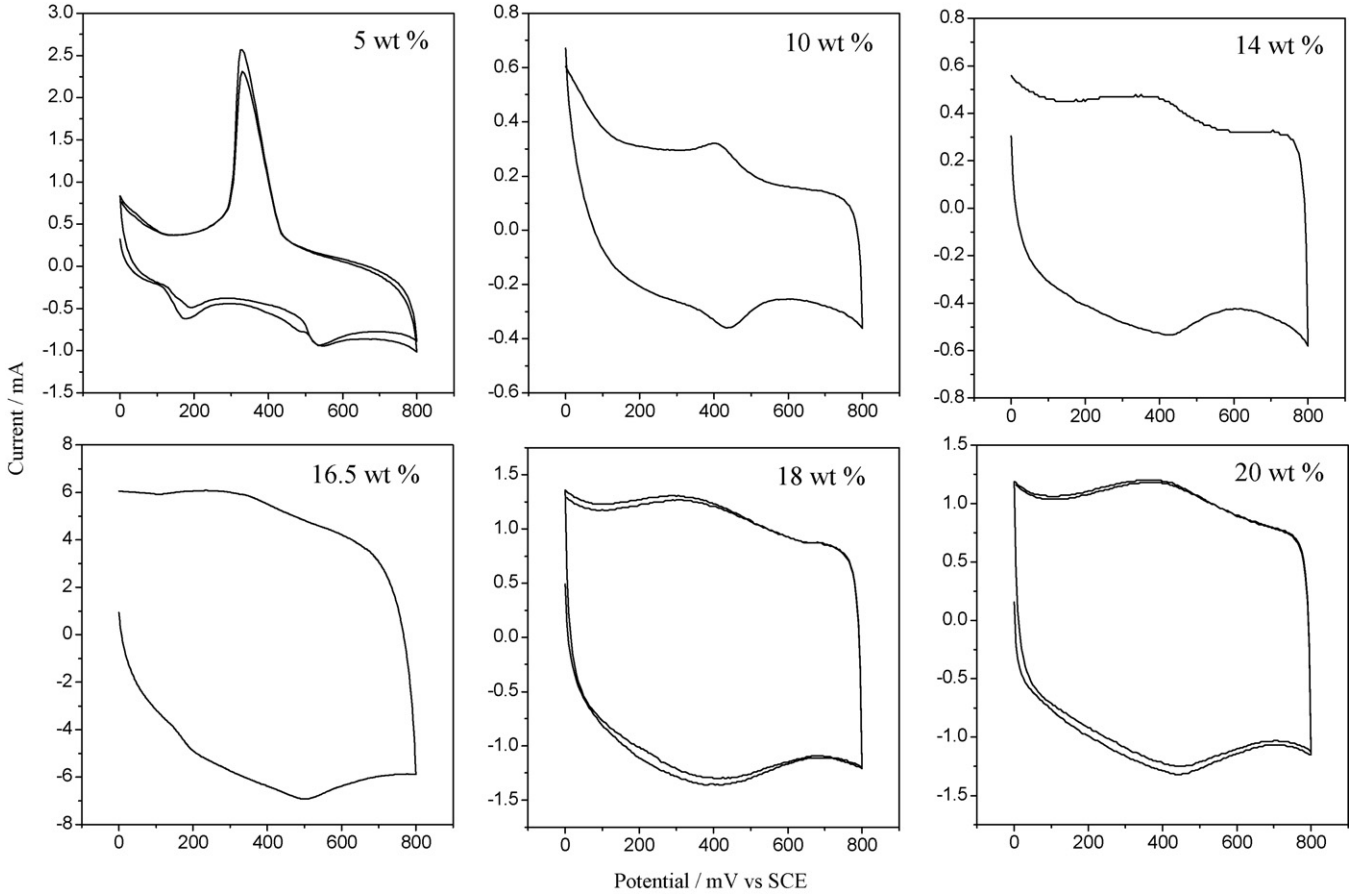

Fig. 6. Cyclic voltammograms of EG–RuO_x composite with different loadings of Ru. The scan rate is 5 mV s^{-1}. Loading of ruthenium oxide in composites given in figure. Potentials are referred to SCE.

device. The 'f_0' can be determined by plotting the resistance (Z') and the reactance (Z'') as a function of frequency (Fig. 4B) and the self-resonance point is a direct measure of f_0 [33,34]. In the present study, the f_0 value varies between 0.05 and 2 Hz for composites with different RuO_x loadings. The reciprocal of the frequency yields the response time of the capacitor. The response time determined for the EG–RuO_x composite is between 0.5 and 12 s. These values are comparable with other commercially available electrochemical capacitors [35].

Fig. 5C represents the normalized imaginary part $|Q|/|S|$ and the real part $|P|/|S|$ of the complex power as a function of frequency. The normalized active power corresponds to the power dissipated [33]. The plot shows that impedance behaviour of a capacitor varies from a pure resistor in the high-frequency region to pure capacitor behaviour in the low-frequency region. A maximum $|Q|/|S|$ is reached in the low-frequency region where the interface behaves like a pure capacitor. The crossing of the plots of $|Q|/|S|$ and $|P|/|S|$ as a function of frequency appears when $|P| = |Q|$, i.e., when $\varphi = 45^\circ$ and $|P|/|S| = |Q|/|S| = 1/\sqrt{2}$, corresponding to the time constant τ_o [33]. Various parameters, such as the nature of the electrolyte solvent and the amount of active material in the electrode, influence the time constant. The time constant is 12 s for the composite containing 16.5 wt.% of RuO_2.

Exfoliated graphite is amenable to intercalation of bisulfate anions when used in the presence of sulfuric acid. The intercalation process is generally observed to be considerable and the material degrades when the acid concentration is very high. The present studies use a low concentration of 0.5 M sulfuric acid. In addition, the RuO_x particles mask the EG surface and these by reduce the available area for intercalation process to give durable composite electrode. Voltammograms of EG–RuO_x composites with different loadings of ruthenium oxide are presented in Fig. 6. The intercalation–deintercalation peaks are very prominent up to a loading of 14 wt.%. The charge–discharge cycles in this range of Ru loading also indicate two processes that correspond to intercalation–deintercalation and the pseudocapacitance associated with the $RuO_x{\cdot}nH_2O$. Intercalation–deintercalation is not observed when a composite of 16.5 wt.% $RuO_x{\cdot}nH_2O$ is used. Hence, further studies are carried out with this composition. The observed capacitance, for 16.5 wt.% $RuO_x{\cdot}nH_2O$ may however, also include a small contribution from the intercalation process.

Typical cyclic voltammograms of the composite containing 16.5 wt.% $RuO_x{\cdot}xH_2O$ are given in Fig. 7A; voltammograms corresponding to the 1st, 100th, 500th and 1000th cycles in 0.5 M H_2SO_4 are shown. The shape and the currents are almost constant during the positive- and negative-going sweeps for a large number of cycles. This indicates that the intercalation of protons inside the RuO_x lattice is fast and reversible. All the composites are quite stable in the aqueous acid electrolyte. The capacitance has also been calculated from the voltammetric response using the equation, $C = [i/\nu m]$ where i, ν and m are the current, scan rate and mass of ruthenium chloride, respectively. It is observed that there is an influence of ruthenium oxide loading on the specific capacitance. With increasing ruthenium oxide loading up to 16.5 wt.% $RuCl_3$, the specific capacitance increases (Fig. 4). Further increase in the Ru loading decreases the specific capacitance. A recent report by Zhang et al. [21] concludes that a loading of 35 wt.% ruthenium on activated carbon (surface area 3000 $m^2\,g^{-1}$) yields a maximum specific capacitance of 750 $F\,g^{-1}$. In the present study, specific capacitances of the order of 176 $F\,g^{-1}$ have been realized with a 16.5 wt.% Ru loading. It should be pointed out that the capacitance values given here are normalized with respect to the mass of the composite used (Fig. 4A) and not to the mass of the active material, RuO_x. The observed capacitance however, includes a contribution from the double-layer capacitance. Ruthenium oxide is reported to generate

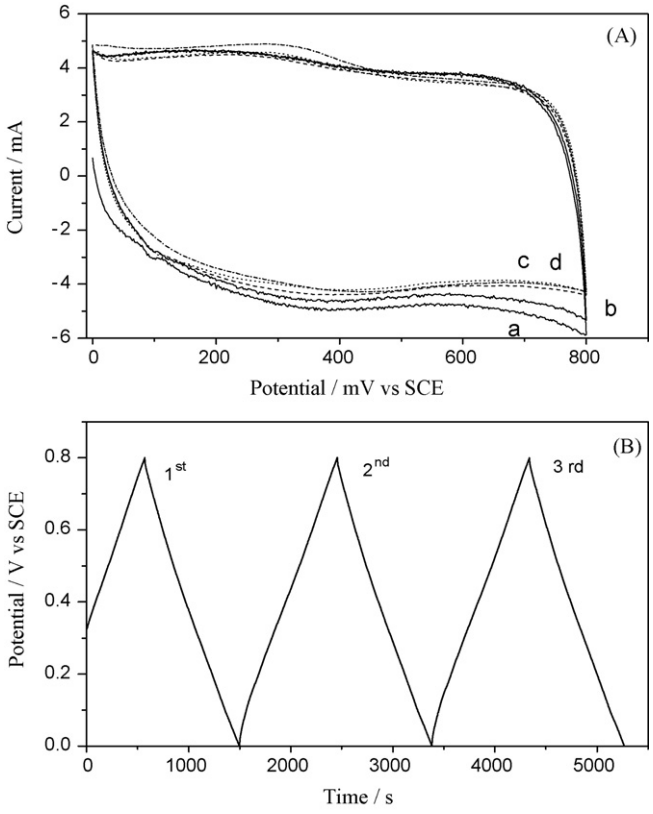

Fig. 7. (A) Cyclic voltammograms of 16.5 wt.% $RuO_x{\cdot}xH_2O$–EG composite in 0.5 M H_2SO_4 at 5 mV s^{-1} scan rate: (a) 1st, (b) 100th, (c) 500th and (d) 1000th cycles. (B) First three cycles of the charge–discharge characteristics at a discharge current density of 1 mA cm^{-2}. Other conditions are as given in Fig. 6.

a high specific capacitance due to the fast and reversible proton intercalation into the lattice [13] according to the reaction:

$$RuO_2 + \delta H^+ + \delta e = RuO_{2-\delta}(OH)_\delta \quad (0 \le \delta \le 2) \tag{1}$$

If it is assumed that all ruthenium is converted to $Ru(OH)_2$ during the electrochemical cycling, then the theoretical capacitance works out to be 1450 $F\,g^{-1}$ with respect to RuO_x [21]. The EG–RuO_x composite would approximately yield thousands of farads per gram of RuO_x when scaled up for the mass of the active material.

Charge–discharge measurements have been performed at different current densities ranging from 1 to 5 mA cm^{-2}. The capacitors are first charged to 0.8 V versus a saturated calomel electrode (SCE) and then discharged to 0 V versus SCE. Fig. 7 shows that typical charge–discharge characteristics of a capacitor fabricated with 16.5 wt.% ruthenium loaded EG at a current density of 1 mA cm^{-2}. A small iR drop of about 11 mV at a current density of 1 mA cm^{-2} is observed at the beginning of discharge. The energy efficiency of a capacitor is given by the ratio of the times taken for the discharging and charging processes and is 98.5% at a current density of 3 mA cm^{-2}.

The ageing and stability of the EG based composites has been tested by storing the electrode material in a vacuum desiccator and monitoring the capacitance characteristics. The behaviour of the composites remains unaltered over a period of almost two years thus showing that the composites have a good storage stability.

4. Conclusions

This study demonstrates the use of exfoliated graphite based composite materials for supercapacitor applications. The EG acts as

a binder as well as an electronic conductor. The composites show very good performance in terms of specific capacitance. This opens up possibilities for preparing composites of EG with various materials including macrocycles and polymers. The EG has a very small number of oxygen-containing functional groups that can exhibit pseudocapacitance.

Acknowledgements

The authors gratefully acknowledge the financial assistance by MNES and DRDO, New Delhi, India. Mr. A. Roychoudhury is thanked for XRD measurements.

References

[1] B.E. Conway, J. Electrochem. Soc. 138 (1991) 1539.
[2] Y. Kibj, T. Saito, M. Kurata, J. Tabuchi, A. Ochi, J. Power Sources 60 (1996) 219.
[3] D. Qu, H. Shi, J. Power Sources 74 (1998) 99.
[4] I. Bispo-Fonseca, J. Aggar, C. Sarrazin, P. Simon, J.F. Fauvarque, J. Power Sources 79 (1999) 238.
[5] A. Yoshida, S. Nonaka, I. Aoki, A. Nishino, J. Power Sources 60 (1996) 207.
[6] V. Srinivasan, J.W. Weidner, J. Electrochem. Soc. 144 (1997) L210.
[7] K.-C. Liu, M.A. Anderson, J. Electrochem. Soc. 143 (1996) 124.
[8] H.Y. Lee, J.B. Goodenough, J. Solid State Chem. 144 (1999) 220.
[9] H.Y. Lee, J.B. Goodenough, J. Solid State Chem. 148 (1999) 81.
[10] C. Lin, J.A. Ritter, B.N. Popov, J. Electrochem. Soc. 145 (1998) 4097.
[11] C.C. Hu, C.H. Chu, J. Electroanal. Chem. 503 (2001) 105.
[12] R. Kortz, M. Carlen, Electrochim. Acta 45 (2000) 2483.
[13] J.P. Zheng, T.R. Jow, J. Electrochem. Soc. 142 (1995) L6.
[14] M. Ramani, B.S. Haran, R.E. White, B.N. Popov, J. Electrochem. Soc. 148 (2001) A374.
[15] Z. Ma, J.P. Zheng, R. Fu, Chem. Phys. Lett. 331 (2000) 64.
[16] E. Frackowiak, F. Bèguin, Carbon 39 (2001) 937.
[17] K. Jurewicz, E. Frackowiak, Mol. Phys. Rep. 27 (2000) 36.
[18] T. Mamma, X. Liu, T. Osaka, Y. Ushio, Y. Sawada, J. Power Sources 60 (1996) 249.
[19] J.P. Zheng, Electrochem. Solid State Lett. 2 (1999) 359.
[20] J.H. Park, O.O. Park, K.H. Shin, C.S. Jin, J.H. Kim, Electrochem. Solid State Lett. 5 (2002) H7.
[21] J. Zhang, D. Jiang, B. Chen, J. Zhu, L. Jiang, H. Fang, J. Electrochem. Soc. 148 (2001) A1362.
[22] G.Z. Chen, M.S.P. Shaffer, D. Coleby, G. Dixon, W. Zhou, D.J. Fray, A.H. Windle, Adv. Mater. 12 (2000) 522.
[23] A. Laforgue, P. Simon, J.F. Fauvarque, J.F. Sarrau, P. Lailler, J. Electrochem. Soc. 148 (2001) A1130.
[24] K. Jurewicz, S. Delpeux, V. Bertagna, F. Beguin, E. Frackowiak, Chem. Phys. Lett. 347 (2001) 36.
[25] J.H. Park, J.M. Ko, O.O. Park, D.-W. Kim, J. Power Sources 105 (2002) 20.
[26] Y.-R. Nian, H. Teng, J. Electrochem. Soc. 149 (2002) A1008.
[27] D.D.L. Chung, J. Mater. Sci. 22 (1987) 4190.
[28] E.P. Gilbert, P.A. Reynolds, J.W. White, J. Chem. Soc., Faraday Trans. 94 (1998) 1861.
[29] (a) K. Fukuda, K. Kikuya, K. Isono, M. Yoshio, J. Power Sources 69 (1997) 165; C.A. Frysz, D.D.L. Chung, Carbon 35 (1997) 858;
(b) C. Wan, K. Azumi, H. Konno, Electrochim. Acta 52 (2007) 3061.
[30] P. Ramesh, S. Sampath, Anal. Chem. 75 (2003) 6949.
[31] R. de Levie, J. Electroanal. Chem. 281 (1990) 1.
[32] M.J. Rodiguez Presa, R.I. Tucceri, M.I. Florit, D. Posadas, J. Electroanal. Chem. 502 (2001) 82.
[33] P.L. Tabrena, P. Simon, J.F. Fauvarque, J. Electrochem. Soc. 150 (2003) A292.
[34] J.R. Miller, in: Pulse performance of electrochemical capacitors, Technical status of present commercial devices, in: Presented at the 8th International Seminar on Double Layer Capacitors and Similar Energy Systems, Florida, 1998.
[35] J.R. Miller, in: F. Delnick, M. Tomkiewicz (Eds.), ECS Symposium, 1996, p. 246.